J Radioanal Nucl Chem (2015) 303:2497–2504
DOI 10.1007/s10967-014-3812-8

Neutron induced reaction cross-section of ^{232}Th and ^{238}U at the neutron energies of 2.45 and 14.8 MeV

H. Naik · S. V. Surayanarayana · S. Bishnoi · T. Patel · A. Sinha · A. Goswami

Received: 29 September 2014 / Published online: 30 November 2014

Abstract For ^{232}Th and ^{238}U, the (n,γ) reaction cross-sections at the neutron energies of 2.45 and 14.8 MeV as well as the (n,2n) reaction cross-sections at 14.8 MeV have been determined using activation and off-line γ-ray spectrometric technique. The (n,γ) and (n,2n) reaction cross-sections of ^{232}Th and ^{238}U were also calculated theoretically using the TALYS 1.6 computer code. The present data and literature data in a wide range of neutron energies were compared with the evaluated data of ENDF/B-VII.1, JENDL-4.0, JEFF-3.1/A and CENDL-3.1 and theoretical value of TALYS to examine the systematics of (n,γ) and (n,2n) reaction cross-sections.

Keywords (n,γ) and (n,2n) reaction cross-sections of ^{232}Th and ^{238}U · D+D and D+T neutrons · Neutron energies of 2.45 ± 0.18 and 14.8 ± 0.1 MeV · Off-line γ-ray spectrometric technique · TALYS calculation

Introduction

Neutron induced reaction and fission cross-sections of isotopes of actinides from Th–Cm are important for various types of reactor applications. In most of the conventional reactors such as light water reactors (PWR, BWR) and heavy water reactor (HWR) in all over the world are based on enriched or natural uranium as the fuel. In all the conventional and fast reactors [1–5], ^{238}U is the major constituents of the fuel. Similarly, in the advanced heavy water reactor (AHWR) [6, 7], ^{232}Th is the important constituents of the fuel. The accelerated driven sub-critical system (ADSs) [8–13] is also advanced reactor used for the incineration of long-lived alpha active minor actinides (^{237}Np, ^{240}Pu, ^{241}Am, ^{243}Am, ^{244}Cm) and transmutation of long-lived fission products (^{93}Zr, ^{99}Tc, ^{107}Pd, ^{129}I, ^{135}Cs). The ADSs [8–13] based on the Th–U fuel cycle is important because one can exploit its potential to design a hybrid reactor system that can produce nuclear power with the use of thorium as main fuel [14]. The ^{232}Th–^{233}U in the oxide form can be used as the primary fuel in AHWR, whereas ^{238}U–^{239}Pu in the form of carbide is used as the primary fuel in fast reactor. The ^{233}U and ^{239}Pu are first generated in a research reactor from ^{232}Th(n,γ)^{233}Th ^{238}U(n,γ)^{239}U reactions and by successive two beta decays. Then the fissile material ^{233}U with ^{232}Th in AHWR and ^{239}Pu with ^{238}U in fast reactor can be used for power generation. The ^{232}Th and ^{238}U are used as the breeding material to regenerate the fissile material ^{233}U and ^{239}Pu, respectively. Thus it is important to have knowledge about the (n,γ) reaction cross-section of ^{232}Th and ^{238}U over a wide range of neutron energy. This is because the range of neutron energy varies from thermal to 15–20 MeV in conventional reactor and from keV to 20 MeV in fast reactor. At higher neutron energy, the (n,2n) reaction of ^{232}Th and ^{238}U are also an important mode of reactions for neutron economy and thus design of different types of reactors.

Sufficient data on the (n,γ) and (n,2n) reaction cross-sections of ^{232}Th [15–44] and ^{238}U [26, 34, 36, 45–73] over

H. Naik (✉) · A. Goswami
Radiochemistry Division, Bhabha Atomic Research Centre, Mumbai 400 085, India
e-mail: naikhbarc@yahoo.com

S. V. Surayanarayana
Nuclear Physics Division, Bhabha Atomic Research Centre, Mumbai 400 085, India

S. Bishnoi · T. Patel · A. Sinha
Neutron and X-ray Physics Facility, Bhabha Atomic Research Centre, Mumbai 400 085, India

a wide range of neutron energy are available in literature based on EXFOR compilation [74]. In the recent past we have determined the (n,γ) and (n,2n) reaction cross-sections of ^{232}Th [41–44] and ^{238}U [70–73] using the wide range of quasi-mono-energetic neutron from the ^{7}Li(p,n) reactions. The ^{232}Th(n,γ) and ^{238}U(n,γ) reaction cross-sections from our earlier work [41–44, 70–73] at the average neutron energy of 3.7 to 17.28 MeV are in good agreement with the calculated data from TALYS [75] as well as evaluated data of ENDF/B-VII.1 [76], JENDL-4.0 [77], JEFF-3.1/A [78] but not with CENDL-3.1 [79] and Ding et al. [80]. However, some of the literature data within the neutron energy of 5–7 MeV [56, 58–60] and 14.2–20 MeV [20, 60, 81] for ^{238}U(n,γ) reaction as well as at 14.5 MeV [20] for ^{232}Th(n,γ) reaction are not in agreement with the calculated data from TALYS [75] and evaluated data of ENDF/BVII [76], JENDL-4.0 [77] and JEFF-3.1[78] but are in agreement with the evaluated data of CENDL-3.1 [79]. In view of this in the present work, the neutron induced reaction cross-sections of ^{232}Th and ^{238}U at the neutron energies of 2.45 and14.8 MeV have been experimentally determined using activation and off-line gamma ray spectrometric technique.

Experimental details

The experiments were carried out using the neutron generator from the Cockcroft and Walton type multiplier accelerator of Purnima at BARC, Mumbai. The Purnima neutron generator is 300 kV DC electrostatic accelerator, in which D^+ ion beam is accelerated at 100 kV and bombarded on deuterium or tritium target of about 6–8 Curie. It produces 2.45 ± 0.18 and 14.8 ± 0.1 MeV mono-energetic neutrons based on the D(d,n)^{3}He ($Q = 3.27$ MeV) and T(d,n)^{4}He ($Q = 17.59$ MeV) reactions, respectively. The operating parameters of the neutron generator for the experiment are 115 μA D^+ ion beam current and vacuum inside the system is maintained at pressure of 3×10^{-6} mbar.

For the neutron energy of 2.45 MeV, 327.5 mg of ^{232}Th, 669.6 mg of ^{238}U metal foil and 207.48 mg of natural In metal foils of about 1 cm^2 size were used for irradiation. The samples were individually wrapped with 0.025 mm thick super pure aluminium foil. A stack of In–Th–U was made from these three samples and mounted at zero degree with respect to the beam direction. The γ-ray activity of ^{115m}In from ^{115}In(n,n′) reaction was used to measure the neutron flux. The isotopic abundance of ^{115}In in natural indium is 95.7 %. The In–Th–U stack was irradiated for 2.5 h with the neutrons beam generated from D + D reaction. In the case of 14.8 MeV neutron irradiation, 285.7 mg of ^{232}Th and 698.0 mg of ^{238}U metal foil of about 1 cm^2 sizes were used for irradiation. The samples were also individually wrapped with 0.025 mm thick aluminium foil and a stack of Th–U was made. The stacks samples were also mounted at zero degree with respect to the beam direction. It was then irradiated for 3.5 h with the neutron beam obtained from the D+T reaction. After irradiation, the samples were cooled for 0.5–1.5 h. Then the irradiated targets of Th, U and In along with Al wrapper were mounted in different Perspex plates and taken for γ-ray spectrometry.

The γ-rays of fission/reaction products from the irradiated Th, U and In samples were counted in an energy and efficiency calibrated 80 c.c. HPGe detector coupled to a PC-based 4 K channel analyzer. The counting dead time was kept always <5 % by placing the irradiated Th, U and In samples at a suitable distance from the detector to avoid pileup effects. The energy and efficiency calibration of the detector system was done by counting the γ-ray energies [82–84] of standard ^{152}Eu and ^{133}Ba sources. The standard ^{152}Eu and ^{133}Ba sources were chosen to cover the energy range from 53.16 to 1408.01 keV to avoid use of so many sources having single or few γ-lines. The efficiency was also determined by using standard sources having one or two γ-lines such as ^{241}Am (59.5 keV), ^{57}Co (122.1, 136.5 keV), ^{137}Cs (661.7 keV), ^{54}Mn (834.5 keV) ^{22}Na (1274.5 keV) and ^{60}Co (1173.2, 1332.5 keV) and found to be in good agreement. The γ-ray counting of the standard sources were done at the same geometry keeping in mind the summation error. The detector efficiency was 20 % at 1332.5 keV γ-ray relative to 3″ diameter ×3″ length NaI(Tl) detector. The uncertainty in the efficiency was 2–3 %. The resolution of the detector system had a FWHM of 1.8 keV at 1332.5 keV γ-ray of ^{60}Co. The γ-ray counting of the irradiated In, Th and U samples were done alternately in the first day. From second day onwards γ-ray counting of only Th and U samples were done up to few months to check the half-life of the nuclides of interest.

Data analysis

Calculation of the neutron flux

In the 2.45 and 14.8 MeV neutron irradiation, the neutron beam was obtained from the D(d,n)^{3}He and T(d,n)^{4}He reactions, respectively. For the 2.45 MeV neutron irradiation, the neutron flux was obtained by using ^{115}In(n,n′)^{115m}In reaction monitor. The observed photo-peak activity (A_{obs}) for 336.2 keV γ-line of ^{115m}In was related to the neutron flux (Φ) with the relation given below [41, 70].

$$\phi = \frac{A_{obs}\left(\frac{CL}{LT}\right)\lambda}{N\sigma_R I_\gamma \varepsilon\left(1-e^{-\lambda t}\right)e^{-\lambda T}\left(1-e^{-\lambda CL}\right)} \quad (1)$$

where N is the number of target atoms and σ_R is the reaction cross-section of the ^{115}In(n, n′)^{115m}In reaction. λ is the decay constant ($\lambda = \ln 2/T_{1/2}$) of the reaction product of interest with half-life = $T_{1/2}$. γ is the branching intensity of the 336.2 keV γ-line of ^{115m}In and ε is its detection efficiency. t, T, CL and LT are the irradiation, cooling, clock and live time, respectively.

For the 14.8 MeV neutron irradiation, the neutron flux (Φ) was obtained from the 529.87 and 1383.93 keV γ-ray activities of the fission product, ^{133}I and ^{92}Sr in both the ^{232}Th(n, f) and ^{238}U(n, f) reactions using the following relation [41, 70].

$$\phi = \frac{A_{obs}\left(\frac{CL}{LT}\right)\lambda}{N\sigma_f I_\gamma \varepsilon Y(1-e^{-\lambda t})e^{-\lambda T}\left(1-e^{-\lambda CL}\right)} \quad (2)$$

All terms in Eq. (2) have the same meaning as in Eq. (1) except the yield (Y) of the fission product and the fission cross-section (σ_f).

In the above two equations, the observed photo-peak activities (A_{obs}) of the 336.2, 529.87 and 1383.93 keV were obtained from the net gross peak-area after subtracting the Compton background [41, 70]. The CL/LT term in Eqs. (1) and (2) has been used for dead time correction. The σ_R for the ^{115}In(n, n′)^{115m}In reaction as well as the σ_f for the ^{232}Th(n, f) and ^{238}U(n, f) reactions were taken from refs [74, 85]. The σ_R value for the ^{115}In(n, n′)^{115m}In reaction at the neutron energy of 2.45 MeV used in the Eq (1) is 0.348 ± 0.019 barn [74, 85]. At the neutron energy of 14.8 MeV, the σ_f values for the ^{232}Th(n,f) and ^{238}U(n,f) reactions [74, 85] used are 0.365 ± 0.034 and 1.249 ± 0.042 barns, respectively. The yield (Y) of the fission products, ^{92}Sr and ^{133}I for the ^{232}Th(n,f) and^{238}-U(n,f) reactions used in the Eq (2) were taken from the refs. [86, 87]. The cumulative yields of ^{92}Sr and ^{133}I in the ^{232}Th(n,f) reaction [86] at the neutron energy of 14 8 MeV were 5.58 ± 0.53 and 3.78 ± 0.18 %, respectively. Similarly, the cumulative yields of ^{92}Sr and ^{133}I in the ^{238}U(n,f) reaction [87] at the neutron energy of 14 8 MeV were 3.87 ± 0.26 and 5.73 ± 0.37 %, respectively. The nuclear spectroscopic data such as half-life ($T_{1/2}$) and branching intensity (a) were taken from refs. [82–84] and are shown in Table 1. However, we have used the nuclear spectroscopic data from Ref. [82] to keep the coherency with our earlier data for the (n,γ) and (n,2n) reaction cross-section of ^{232}Th [41–44] and ^{238}U [70–73]. The neutron fluxes were then calculated from Eqs. (1) and (2) by using different terms. The neutron flux obtained from the γ-ray activity of ^{115m}In from the ^{115}In(n,n') reaction for 2.45 MeV neutron irradiation is (1.526 ± 0.180) × 10^5 n cm^{-2} s^{-1}.

Table 1 Nuclear spectroscopic data used in the calculation from refs. [82, 83]

Nuclide	Half-life	γ-ray energy (keV)	γ-ray abundance (%)
^{92}Sr	2.71 h	**1383.93**	**90.0**
^{133}I	20.8 h	**529.87**	**87.0**
^{115m}In	4.486 h	**336.2**	**45.9**
^{231}Th	25.52 h	84.22	6.6
^{233}Th	22.3 m	86.48	2.7
^{233}Pa	26.967 days	300.34	6.62
		312.17	**38.6**
		340.81	4.47
^{237}U	6.75 days	101.06	25.4
		208.0	**21.2**
^{239}U	23.45 m	74.66	48.0
^{239}Np	2.3565 days	103.73	24.2
		106.13	27.2
		209.75	3.42
		228.18	10.76
		277.6	**14.38**

The γ-ray energy and their branching intensity marked with bold letters are used for calculations

Similarly, the average neutron flux obtained from the fission products (^{92}Sr and ^{133}I) activities of the ^{232}Th(n,f) and^{238}U(n,f) reactions for the 14.8 MeV neutron irradiation is (3.108 ± 0.077) × 10^5 n cm^{-2} s^{-1}.

Determination of (n, γ) and (n, 2n) reaction cross-sections of ^{232}Th and ^{238}U

The nuclear spectroscopic data used in the present work for the calculation of the (n,γ) and (n,2n) reaction cross-sections of ^{232}Th and ^{238}U are taken from the refs. [82–84] and are given in Table 1. In the case of ^{232}Th(n, γ) reaction, the half-life of the reaction product, ^{233}Th is 22.3 min, which decays 99.61 % to ^{233}Pa within 3 h. In view of this, the ^{232}Th(n, γ) cross-section was calculated from the observed photo-peak activity of ^{233}Pa ($T_{1/2}$ = 26.967 days) of the long cooled spectrum. In the calculation, the photo-peak activity of the 312.2 keV γ-line was used instead of 300.3 keV. This is to avoid the interference of the 300.1 keV γ-line of ^{212}Pb, which is the decay product from ^{232}Th. Similarly, the ^{232}Th(n,2n) reaction cross-section was calculated from the observed activity of the 84.2 keV γ-line of ^{231}Th ($T_{1/2}$ = 25.52 h) from the γ-ray spectrum of a sufficiently cooled sample. This is because in the gamma ray spectrum recorded within 3–4 h, the γ-line of 84.2 keV of ^{231}Th has the interference from the 86.5 keV of ^{233}Th ($T_{1/2}$ = 22.3 min). The observed photo-peak activities (A_{obs}) of the 84.2 keV γ-line for ^{231}Th and the 312.2 keV γ-line for ^{233}Pa are related to the ^{232}Th(n,γ) and ^{232}Th(n,2n)

reaction cross-section (σ) with the following relation [41, 70].

$$\sigma_R = \frac{A_{obs}\left(\frac{CL}{LT}\right)\lambda}{N\phi I_\gamma \varepsilon (1 - e^{-\lambda t})e^{-\lambda T}(1 - e^{-\lambda CL})} \quad (3)$$

All terms in Eq. (3) have the same meaning as in Eq. (1). The neutron flux (Φ) of (1.526 ± 0.180) × 10^5 n cm^{-2} s^{-1} was used to calculate the ^{232}Th(n,γ) reaction cross-section at neutron energy of 2.45 MeV, which is 36.396 ± 4.571 mb. Similarly, at neutron energy of 14.8 MeV, the neutron flux (Φ) of (3.108 ± 0.077) × 10^5 n cm^{-2} s^{-1} was used to calculate the ^{232}Th(n,γ) and ^{232}Th(n,2n) reaction cross-sections, which are 1.569 ± 0.257 and 1674.0 ± 92.0 mb, respectively.

In the case of ^{238}U(n, γ) reaction, the half-life of ^{239}U is 23.54 min (Table 1), which decays 99.6 % to ^{239}Np within 3 h. In view of this, the ^{238}U(n,γ) reaction cross-section (σ_R) was calculated from the γ-ray activity of ^{239}Np ($T_{1/2}$ = 2.3565 days) measured after sufficient cooling time. In the calculation, the photo-peak activity of the 277.6 keV γ-line was used instead of 228.18 keV. This is to avoid the interference of the 228.16 keV γ-line of the fission product ^{132}Te ($T_{1/2}$ = 3.204 days), which comes from ^{238}U(n,f) reaction. Similarly, the ^{238}U(n,2n) reaction cross-section was calculated from the observed activity of the 208.0 keV γ-line of ^{237}U obtained from the γ-ray spectrum of a sufficiently cooling time, when ^{239}U could not be detected any more. This is because ^{239}Np has the 209.75 keV interfering γ-lines. The photo-peak activity of the γ-line 208.0 keV instead of 101.06 keV was used in the calculation because the fission product ^{153}Sm ($T_{1/2}$ = 46.284 h) from ^{238}U(n,f) reaction has an interfering γ-line of 103.18 keV. The observed photo-peak activities (A_{obs}) of the 208.0 keV γ-line for ^{237}U and the 277.6 keV γ-line for ^{239}Np were used in Eq. (3) for the calculation of (n, γ) and (n, 2n) reaction cross-sections (σ_R) of the ^{238}U. The neutron flux (Φ) of (1.526 ± 0.180) × 10^5 n cm^{-2} s^{-1} at neutron energy of 2.45 MeV was used to calculate the ^{238}U(n, γ) reaction cross-section, which is 30.004 ± 4.284 mb. Similarly, at neutron energy of 14.8 MeV, the neutron flux (Φ) of (3.108 ± 0.077) × 10^5 n cm^{-2} s^{-1} was used to calculate the ^{238}U(n, γ) and ^{238}U(n, 2n) reaction cross-sections, which are 1.266 ± 0.379 and 692.7 ± 28.7 mb, respectively.

Results and discussion

The neutron flux used in the calculation as well as the (n,γ) and (n,2n) reaction cross-sections of ^{232}Th and ^{238}U at neutron energies of 2.45 and 14.8 MeV from the present work are given in Table 2. In the same table, the literature data from refs [20, 81] and evaluated data from ENDF/B-VII.1 [76], JENDL-4.0 [77], JEFF-3.1/A [78] and CENDL-3.1 [79] are also given for comparison. The uncertainties associated to the measured cross-sections are from the replicate measurements. The overall uncertainty is the quadratic sum of both statistical and systematic uncertainties. The random error in the observed activity is primarily due to counting statistics, which is estimated to be 10–15 %. This can be determined by accumulating the data for an optimum time period that depends on the half-life of the nuclides of interest. The systematic errors are due to uncertainties in the irradiation time (~0.25 %), the detection efficiency calibration (~3 %), the half-life of the fission products and the γ-ray abundances (~2 %) as reported in the literature [82–84]. Besides this, systematic errors are due to the uncertainty in the neutron flux estimation (~15.7 %) at the neutron energy of 2.45 MeV and (~2.6 %) at 14.8 MeV. Similarly, the uncertainty during the flux determination also comes from the uncertainty in the σ_R value of ^{115}In(n,n′)^{115m}In reaction (~0.7 %) at neutron energy of 2.45 MeV and in the σ_f value of ^{232}Th(n,f) reaction (9.3 %) and ^{238}U(n,f) reaction (3.4 %) at 14.8 MeV. Thus, the total systematic errors are different for the (n,γ) and (n,2n) reaction cross-sections of ^{232}Th and ^{238}U at the neutron energies of 2.45 and 14.8 MeV. The systematic uncertainty for the (n,γ) and the (n,2n) reaction cross-sections of ^{232}Th and ^{238}U is ~16.1 % at the neutron energy of 2.45 MeV and ~5–10 % at 14.8 MeV. Thus the overall uncertainty is found to be ~16–19 %, coming from the statistical and systematic uncertainties at the neutron energies of 2.45 and 14. 8 MeV.

The experimental data of present work from Table 2 and literature data [15–74] as well as the evaluated data from different compilations [76–80] for the (n,γ) and (n,2n) reactions of ^{232}Th and ^{238}U were plotted in Figs. 1, 2, 3 and 4 for comparison. It can be seen from Table 2 and Figs. 1 and 2 that the experimental (n,γ) reaction cross-sections of ^{232}Th and ^{238}U at neutron energy of 2.45 MeV and (n,2n) reaction cross-sections at 14.8 MeV from the present work are in good agreement with the literature data [74] and evaluated data of ENDF/B-VII.1 [76], JENDL-4.0 [77], JEFF-3.1/A [78] and CENDL [79]. However, the (n,γ) reaction cross-sections of ^{232}Th and ^{238}U at neutron energy 14.8 MeV from the present experiment are significantly lower than the literature data [20] but are in agreement with the evaluated data from CENDL-3.1 [79] and slightly higher than the evaluated data from ENDF/B-VII.1 [76], JENDL-4.0 [77], JEFF-3.1/A [78] and Ding et al. [80] compilation. In order to examine this aspect, the (n,γ) and (n,2n) reaction cross-sections of ^{232}Th and ^{238}U at different neutron energy beyond 1 keV were also calculated theoretically using the computer code TALYS, version 1.6 [75]. TALYS [75] can be used to calculate the reaction cross-section based on physics models and parameterizations. It calculates nuclear reactions involving targets with mass

Table 2 The (n, γ) and (n, 2n) reaction cross-sections of ^{232}Th and ^{238}U at neutron energy of 2.45 ± 0.18 and 14.8 ± 0.1 MeV

Systems	Neutron energy (MeV)	Neutron flux (n cm^{-2} s^{-1})	Expt. cross-section (mb)	ENDF cross-section (mb)	JENDL cross-section (mb)	JEF-3.1/A cross-section (mb)	CENDL-4.0 cross-section (mb)
^{232}Th(n,γ)	2.45 ± 0.18	(1.53 ± 0.18) × 10^5	36.396 ± 4.571	49.457–45.170	48.781–43.491	42.000	42.770–37.900
^{232}Th(n,γ)	14.8 ± 0.1	(3.11 ± 0.08) × 10^5	1.569 ± 0.257	1.154–1.007	1.136–1.059	1.500	1.657–1.683
^{232}Th(n,2n)	14.8 ± 0.1	(3.11 ± 0.08) × 10^5	1674.0 ± 92.0	1148.1–985.8	1515.1–1295.2	1258.9–1191.2	1271.6–1149.6
^{238}U(n,γ)	2.45 ± 0.18	(1.53 ± 0.18) × 10^5	30.004 ± 4.284	38.500–27.939	33.887–31.374	31.200	32.256–29.717
^{238}U(n,γ)	14.8 ± 0.1	(3.11 ± 0.08) × 10^5	1.266 ± 0.379	0.880–0.710	0.536–0.469	0.880	1.263–1.564
^{238}U(n,2n)	14.8 ± 0.1	(3.11 ± 0.08) × 10^5	692.7 ± 28.7	719.5–593.8	817.5–682.0	704.0–589.7	629.0

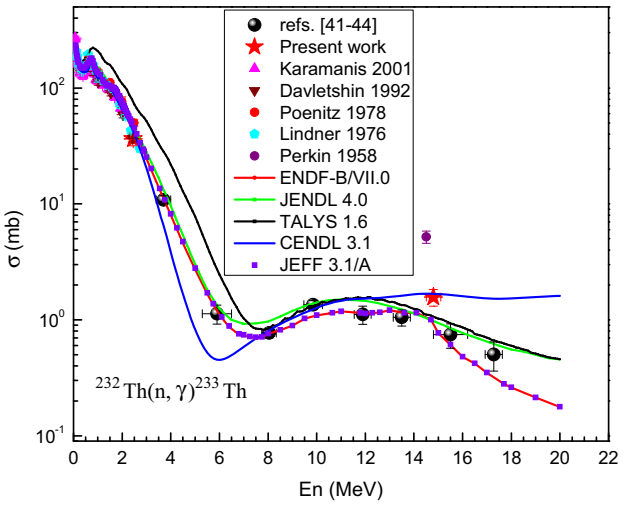

Fig. 1 *Plot* of the experimental and evaluated ^{232}Th(n, γ) reaction cross-section as a function of the neutron energy from 1 to 20 MeV. Experimental values from the present work and from refs. [15–31, 41–44] are in *different symbols*, whereas the evaluated and theoretical values from TALYS are in *solid lines* of *different colours*

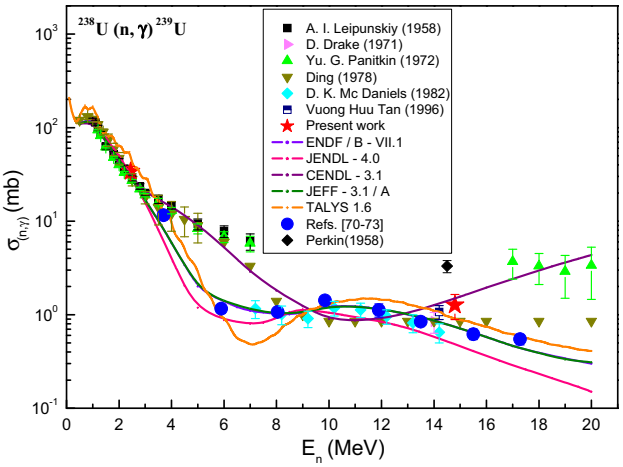

Fig. 2 *Plot* of the experimental and evaluated ^{238}U(n, γ) reaction cross-section as a function of the neutron energy from 1 to 20 MeV. Experimental values from the present work and from refs. [45–60, 70–73] are in *different symbols*, whereas the evaluated and theoretical values from TALYS are in *solid lines* of *different colours*

larger than 12 amu and projectiles like photon, neutron, proton, ^{2}H, ^{3}H, ^{3}He and alpha particles in the energy range from 1 to 200 MeV. In the present work, we have used neutron energies from 1 to 20 MeV for the ^{232}Th and ^{238}U target. All possible outgoing channels for a given projectile (neutron) energy were considered including inelastic and fission channels. However, the cross-sections for the (n, γ) and (n, 2n) reactions were specially looked for and collected.

The calculated (n γ) reaction cross-sections of ^{232}Th and ^{238}U from TALYS are plotted in Figs. 1 and 2 as a function of neutron energy from 100 to 20 MeV. On the other hand, the calculated (n,2n) reaction cross-sections of ^{232}Th and ^{238}U from TALYS are plotted in Figs. 3 and 4 as a function of neutron energy. It can be seen from Figs. 1 and 2 that the (n,γ) reaction cross-sections of ^{232}Th and ^{238}U from TALYS [75] and the evaluated data from ENDF/B-VII.1 [76], JENDL-4.0 [77], JEFF-3.1/A [78] follows the same trend

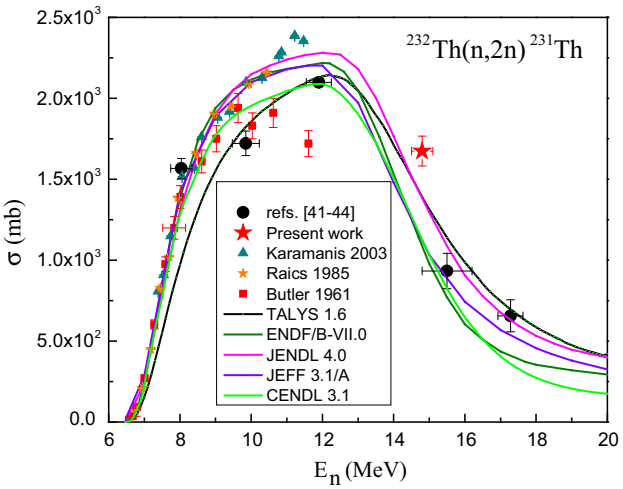

Fig. 3 *Plot* of the experimental and evaluated ^{232}Th(n, 2n) reaction cross-section as a function of the neutron energy from 5 to 20 MeV. Experimental values from the present work and from refs. [32–44] are in *different symbols*, whereas the evaluated and theoretical values from TALYS are in *solid lines* with *different colours*

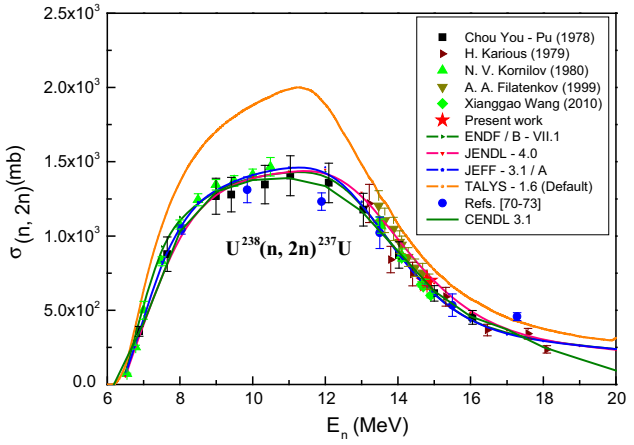

Fig. 4 *Plot* of the experimental and evaluated ^{238}U(n, 2n) reaction cross-section as a function of the neutron energy from 5 to 20 MeV. Experimental values from the present work and from refs. [53, 61–73] are in *different symbols*, whereas the evaluated and theoretical values from TALYS are in *solid lines* with *different colours*

but not the evaluated data from CENDL-3.1 [79] and Ding et al. [80]. It can be also seen from Figs. 1 and 2 that the experimental (n,γ) reaction cross-sections of ^{232}Th and ^{238}U from literature [20, 60] within neutron energy of 14.8–18.1 MeV are significantly higher than the calculated values from TALYS and evaluated data from ENDF/B-VII.1 [76], JENDL-4.0 [77], JEFF-3.1/A [78] and Dinge et al. [80]. However, the evaluated cross-section data of CENDL-3.1 [79] for ^{238}U(n,γ) reaction is in agreement with the literature data within neutron energy of 16.5–18.1 MeV [60] but not at 14.8 MeV [20]. The present data at 14.8 MeV and our earlier data [41–44, 70–73] within neutron energy of 5.9–15.5 MeV follow the trend of the calculated values from TALYS and evaluated data from ENDF/B-VII.1 [76], JENDL-4.0 [77], JEFF-3.1/A [78]. The data within neutron energy of 5.9-15.5 MeV from our earlier work were obtained by using the neutrons from the ^{7}Li(p,n) reaction, in which correction for the cross-section due to the tail part of the neutron spectrum was taken care [41–44, 70–73]. Thus the significantly higher (n,γ) reaction cross-sections of ^{232}Th and ^{238}U within the neutron energies of 14.8–18.1 MeV from literature [20, 60] is most probably due to the contribution of cross-sections from the low energy scattered neutrons. This indicates that the tail part of the neutron spectrum [41–44, 70–73] or the scattered neutron effect the (n,γ) reaction cross-sections of ^{232}Th and ^{238}U. This is evident from the (n,2n) reaction cross-sections of ^{232}Th and ^{238}U of Figs. 3 and 4, where the experimental data of present work and literature [32–44, 53, 61–73] follows the same trend of evaluated data [76–78] and calculated data of TALYS [75]. This is because the low energy tail part of the neutron spectrum [41–44, 70–73] or the low energy scattered neutron does not contribute significantly to the (n,2n) reaction due to its threshold value of 6.25–6.4 MeV.

Leaving behind the above discrepancy and resonance cross-section, one can see from Figs. 1 and 2 that the (n,γ) reaction cross-sections of ^{232}Th and ^{238}U decreases from the neutron energy of 100 keV to 6–7 MeV based on the 1/V trend. Around neutron energy of 6–7 MeV, where the (n,2n) reaction cross-section of ^{232}Th and ^{238}U start increasing, the (n,γ) reaction cross-section remains minimum. Above 8 MeV, where the (n,2n) reaction cross-sections of ^{232}Th and ^{238}U remain constant, the (n,γ) reaction cross-section again increases. Within neutron energy of 8–14 MeV both the (n,γ) and (n,2n) reaction cross-sections of ^{232}Th and ^{238}U remain almost constant. However, above neutron energy of 12–14 MeV, both the (n,γ) and (n,2n) reaction cross-sections of ^{232}Th and ^{238}U starts decreasing due to the opening of (n,3n) reaction channels. These observations indicate the partition of excitation energy in different reaction channels besides (n,f) degrees of freedom.

Conclusion

(i) The ^{232}Th(n,γ) and ^{238}U(n,γ) reaction cross-sections at neutron energy of 2.45 and 14.8 MeV are determined using off-line gamma ray spectrometric technique. The ^{232}Th(n,2n) and ^{238}U(n,2n) reaction cross-sections at neutron energy of 14.8 MeV are also determined using the same technique.

(ii) The (n,γ) and (n,2n) reaction cross-sections of ^{232}Th and ^{238}U at neutron energy of 2.45 and 14.8 MeV were also calculated using computer code TALYS 1.4. The (n,γ) reaction cross-sections at neutron energy of 2.45 MeV and (n,2n) reaction cross-section at 14.8 MeV are in good agreement with the literature data, evaluated data of ENDF/B-VII.1, JENDL-4.0 and JEFF-3.1/A as well as with the calculated values from TALYS. However, the ^{232}Th(n,γ) and ^{238}U(n,γ) reaction cross-sections at neutron energy of 14.8 MeV are slightly higher than the calculated values from TALYS and the evaluated data of ENDF/B-VII.1, JENDL-4.0, JEFF-3.1/A but are in agreement with the data of CENDL 3.1.

Acknowledgments The authors are thankful to the staff of PURNIMA for their excellent operation of the neutron generator and kind cooperation to provide the neutron beam to carry out the experiment.

References

1. Allen TR, Crawford DC (2007) Science and technology of nuclear installations

2. MacDonald PE, Todreas N (2000) Annual project status report 2000, MIT-ANP-PR-071, INEFL/EXT-2009-00994
3. Mathieu L, Heuer D, Brissot R, Garzenne C, Le Brun C, Lecarpentier D, Liatard E, Loiseaux JM, Méplan O, Merle-Lucotte E, Nuttin A (2005) Proposal for a simplified thorium molten salt reactor: In Proceedings of the global international conference, Paper No 428, Tsukuba, Japan
4. Nuttin A, Heuer D, Billebaud A, Brissot R, Le Brun C, Liatard E, Loiseaux JM, Mathieu L, Meplan O, Merle-Lucotte E, Nifenecker H, Perdu F, David S (2005) Proc Nucl Energy 46(1):77–99
5. Fast Reactors and Accelerator Driven Systems Knowledge Base, IAEA-TECDOC-1319: Thorium fuel utilization: options and trends
6. Sinha RK, Kakodkar A (2006) Design and development of AHWR: the Indian thorium fueled innovative reactor. Nucl Eng Des 236(7):683–700
7. Ganesan S (2006) Third research co-ordination meeting, Vienna, Austria, INDC (NDS)-0494
8. Carminati F, Klapisch R, Revol JP, Rubia JA, Rubia C (1993), CERN/AT/93-49 (ET)
9. Rubia C, Rubio JA, Buono S, Carminati F, Fietier N, Galvez J, Geles C, Kadi Y, Klapisch R, Mandrilion P, Revol JP, Roche Ch (1995) CERN/AT/95-44(ET); (1995) CERN/AT/95-53(ET), (1996) CERN/LHC/96-01(LET), (1997) CERN/LHC/97-01(EET)
10. Bowman CD (1994) AIP Conf. Proc. 346, Proceeding of international conference on accelerator-driven transmutation technologies and applications, Las Vegas, NV
11. Accelerator Driven Systems: Energy Generation and Transmutation of Nuclear Waste, Status report (Nov. 1997) IAEA, Vienna, IAEA-TECDO-985
12. Bowman CD (1998) Ann Rev Nucl Part Sci 48:505–556
13. Ganesan S (2007) Pramana (J Phys) 68(2):257–268
14. Kapoor SS (2002) Pramana (J Phys) 59(6):941–950
15. Little RC, Block RC, Harris DR, Slovacek RE, Carlson ON (1981) Nucl Sci Eng 79:175–183
16. Borella A, Volev K, Brusegan A, Schillebeeckx P, Corvi F, Koyumdjieva N, Janeva N, Lukyanov AA (2006) Nucl Sci Eng 152:1–14
17. Aerts G, Abbondanno U, Álvarez H, Alvarez-Velarde F, Andriamonje S, Andrzejewski J, Assimakopoulos P, Audouin L, Badurek G, Baumann P, Běcvář F, Berthoumieux E, Calvĩno F, Cano-Ott D, Capote R, Carrillo de Albornoz A, Cennini P, Chepel V, Chiaveri E, Colonna N, Cortes G, Couture A, Cox J, Dahlfors M, David S, Dillman I, Dolfini R, Domingo-Pardo C, Dridi W, Duran I, Eleftheriadis C, Embid-Segura M, Ferrant L, Ferrari A, Ferreira-Marques R, Fitzpatrick L, Frais-Koelbl H, Fujii K, Furman W, Goncalves I, Gonzalez-Romero E, Goverdovski A, Gramegna F, Griesmayer E, Guerrero C, Gunsing F, Haas B, Haight R, Heil M, Herrera-Martinez A, Igashira M, Isaev S, Jericha E, Ǩappeler F, Kadi Y, Karadimos D, Karamanis D, Kerveno M, Ketlerov V, Koehler P, Konovalov V, Kossionides E, Krtǐcka M, Lamboudis C, Leeb H, Lindote A, Lopes I, Lozano M, Lukic S, Marganiec J, Marques L, Marrone S, Mastinu P, Mengoni A, Milazzo PM, Moreau C, Mosconi M, Neves F, Oberhummer H, O'Brien S, Oshima M, Pancin J, Papachristodoulou C, Papadopoulos C, Paradela C, Patronis N, Pavlik A, Pavlopoulos P, Perrot L, Pigni MT, Plag R, Plompen A, Plukis A, Poch A, Pretel C, Quesada J, Rauscher T, Reifarth R, Rosetti M, Rubbia C, Rudolf G, Rullhusen P, Salgado J, Sarchiapone L, Savvidis I, Stephan C, Taliente G, Tain JL, Tassan-Got L, Tavora L, Terlizzi R, Vannini G, Vaz P, Ventura A, Villamarin D, Vincente MC, Vlachoudis V, Vlastou R, Voss F, Walter S, Wendler H, Wiescher M, Wisshak K (2006) Phys Rev C 73:054610
18. Pomerance H (1952) Phys Rev 88:412–413
19. Macklin RL, Lazar NH, Lyon WS (1957) Phys Rev 107:504–508
20. Perkin JL, O'Connor LP, Colemann RF (1958) Proc Phys Soc 72:505–513
21. Miskel JA, Marsh KV, Lindner M, Nagle RJ (1962) Phys Rev 128:2717–2723
22. Stupegia DC, Smith B, Hamm K (1963) J Inorg Nucl Chem 25:627–630
23. Muxon MC (1963) TRDWP/P-8 (U.K. Atomic Energy Authority, Harwell)
24. Forman L, Schelberg AD, Warren JH, Glass NW (1971) Phys Rev Lett 27:117–120
25. Chelnokov VB et al (Oct 1972) USSR Obninsk Report, Jaderno Fizicheskii Issledovanija No. 13, page 6
26. Lindner M, Nagle RJ, Landrum JH (1976) Nucl Sci Eng 59:381–394
27. Chrien RE, Liou HI, Kenny MJ, Stelts ML (1979) Nucl Sci Eng 72:202–215
28. Baldwin GT, Knoll GF (1984) Nucl Sci Eng 88:123–128
29. Jones RT, Merritt JS, Okazaki A (1986) Nucl Sci Eng 93:171–180
30. Wisshak K, Voss F, Kappeler F (2001) Nucl Sci Eng 137:183–193
31. Karamanis D, Petit M, Andriamonje S, Barreau G, Bercion M, Billebaud A, Blank B, Czajkowski S, Del Moral R, Giovinazzo J, Lacoste V, Marchand C, Perrot L, Pravikoff M, Thomas JC (2001) Nucl Sci Eng 139:282–292
32. Prestwood RJ, Bayhurst BP (1961) Phys Rev 121:1438–1441
33. Butler JP, Santry DC (1961) Can J Chem 39:689–696
34. Batchelor R, Gilboy WB, Towle JH (1965) Nucl Phys 65:236–256
35. Bormann M (1965) Nucl Phys 65:257–274
36. Karius H, Ackermann A, Scobel W (1979) J Phys G 5:715–721
37. Chatani H (1983) Nucl Instrum Methods 205:501–504
38. Raics P, Daroczy S, Csikai J, Kornilov NV, Baryba VYa, Salnikov OA (1985) Phys Rev C 32:87–91
39. Karamanis D, Andriamonje S, Assimakopoulos PA, Dourkellis G, Karademos DA, Karydas A, Kokkoris M, Korrssionides S, Nicolis NG, Papachristodoulou C, Papadopoulos CT, Patronis N, Pavlopulous P, Perdikakis G, Vlastos R (2003) Nucl Instrum Methods Phys Res A 505:381–384
40. Reyhancan IA (2011) Ann Nucl Energy 38:2359–2362
41. Naik H, Prajapati PM, Surayanarayana SV, Jagadeesan KC, Thakare SV, Raj D, Mulik VK, Sivashankar BS, Nayak BK, Sharma SC, Mukherjee S, Singh S, Goswami A, Ganesan S, Manchanda VK (2011) Eur Phys J A 47:51–60
42. Prajapati PM, Naik H, Suryanarayana SV, Mukherjee S, Jagadeesan KC, Sharma SC, Thakre SV, Rasheed KK, Ganesan S, Goswami A (2012) Eur Phys J A 48:35–42
43. Rita C, Naik H, Suryanarayana SV, Shivashankar BS, Mulik VK, Prajapati PM, Sanjeev G, Sharma SC, Bhagwat PV, Mohanty AK, Ganesan S, Goswami A (2012) Ann Nucl Energy 47:160–165
44. Mukerji S, Naik H, Suryanarayana SV, Chachara S, Shivasankar BS, Mulik VK, Crasta R, Samanta S, Nayak BK, Saxena A, Sharma SC, Bhagwat PV, Rasheed KK, Jindal RN, Ganesan S, Mohanty AK, Goswami A, Krishani PD (2012) Pramana J Phys 79:249–262
45. Diven BC, Terrell J, Hemmendinger A (1960) Phys Rev 120:556–569
46. Asghar M, Chaffey CM, Moxon MC (1966) Nucl Phys 85:305–316
47. Menlove HO, Poenitz WP (1968) Nucl Sci Eng 33:24–30
48. Drake D, Bergqvist I, McDaniels DK (1971) Phys Lett B 36:557–559
49. De Saussure G, Silver EG, Perez RB, Ingle R, Weaver H (1973) Nucl Sci Eng 51:385–404
50. Poenitz WP (1975) Nucl Sci Eng 57:300–308
51. Liou HI, Chrien RE (1977) Nucl Sci Eng 62:463–478

52. Wisshak K, Kappeler F (1978) Nucl Sci Eng 66:363–377
53. Perez RB, de Saussure G, Macklin RL, Halperin J (1979) Phys Rev C 20:528–545
54. Mc Daniels DK, Varghese P, Drake DM, Arthur F, Lindholm A, Berquist I, Krumlinde J (1982) Nucl Phys A 384:88–96
55. Voignier J, Joly S, Grenier G (1992) Nucl Sci Eng 112:87–94
56. Leipunskiy AI, Kazachkovskiy OD, Artyukhov GJa, Baryshnikov AI, Belanova TS, Galkov VI, Stavisskiy YuJa, Stumbur EA, Sherman LE (1958) 58GENEVA 15:50
57. Barry JF, Bunce J, White PH (1964) J Nucl Energy A&B (Reactor Sci and Technol) 18:481–489
58. Panitkin YuG, Tolstikov VA (1972) Atomnaya Energia 33:782–783
59. Panitkin YuG, Tolstikov VA (1972) Atomnaya Energia 33:825–827
60. Panitkin YuG (1975) Tolstikov VA. Atomnaya Energia 39:17–19
61. Poenitz WP, Fawcell LR Jr, Smith DL (1981) Nucl Sci Eng 78:239–247
62. Buleeva NN, Davletshin AN, Tipunkov OA, Tikhonov SV, Tolstokov VA (1988) Atomnaya Energia 65:348–352
63. Quang E, Knoll GF (1991) Nucl Sci Eng 110:282–288
64. Perkin JL, Coleman RF (1961) J Nucl Energy A&B (Reactor Sci and Technol) 14:69–75
65. Landrum JH, Nagle RJ, Lindner M (1973) Phys Rev C 8:1938–1944
66. Frchaut J, Bertin A, Bois R (1980) Nucl Sci Eng 74:29–33
67. Kornilov NV, Zhuravlev BV, Sal'nikov OA, Raich P, Nad' Sh, Darotsi Sh, Sailer K, Chikai I (1980) Atomnaya Energia 49:283–286
68. Shani G (1983) Ann Nucl Energy 10:473–476
69. Wang X, Jiang S, He M, Dong K, Xiao C (2010) Nucl Instrum Methods Phys Res A 621:326–330
70. Naik H, Suryanarayana SV, Mulik VK, Prajapati PM, Shivashankar BS, Jagadeesan KC, Thakare SV, Raj D, Sharma SC, Bhagwat PV, Dhole SD, Bhoraskar VN, Goswami A (2012) J Radioanal Nucl Chem 293:469–478
71. Sadhana M, Naik H, Surayanarayana SV, Shivashankar BS, Mulik VK, Chachara Sachin, Samanta Sudipta, Goswami A, Krishnani PD (2013) J Basic Appl Phys 2:104–113
72. Mulik VK, Surayanarayana SV, Naik H, Mukerji Sadhana, Shivashankar BS, Prajapati PM, Dhole SD, Bhoraskar VN, Ganesan S, Goswami A (2014) Annal Nucl Energy 63:233–240
73. Crasta R, Ganesh S, Naik H, Goswami A, Suryanarayana SV, Sharma SC, Bhagwat PV, Shivashankar BS, Mulik VK, Prajapati PM (2014) Nucl Sci Eng 178:1–10
74. Otuka N, Dupont E, Semkova V, Pritychenko B, Blokhin AI, Aikawa M, Babykina S, Bossant M, Chen G, Dunaeva S, Forrest RA, Fukahori T, Furutachi N, Ganesan S, Ge Z, Gritzay OO, Herman M, Hlavăc S, Kato K, Lalremruata B, Lee YO, Makinaga A, Matsumoto K, Mikhaylyukova M, Pikulina G, Pronyaev VG, Saxena A, Schwerer O, Simakov SP, Soppera N, Suzuki R, Takács S, Tao X, Taova S, Ťarkanyi F, Varlamov VV, Wang J, Yang SC, Zerkin V and Zhuang Y (2014) Nucl Data Sheets 120:272–276 (IAEA-EXFOR Database. http://www-nds.iaea.org/exfor)
75. Koning AJ, Rochman D (2012) Modern nuclear data evaluation with the TALYS code system. Nucl Data Sheets 113:2841
76. Chadwick MB, Obložinský PM, Herman M, Greene NM, McKnight RD, Smith DL, Young PG, MacFarlane RE, Hale GM, Frankle SC, Kahler AC, Kawano T, Little RC, Madland DG, Moller P, Mosteller RD, Page PR, Talou P, Trellue H, White MC, Wilson WB, Arcilla R, Dunford CL, Mughabghab SF, Pritychenko B, Rochman D, Sonzogni AA, Lubitz CR, Trumbull TH, Weinman JP, Brown DA, Cullen DE, Heinrichs DP, McNabb DP, Derrien H, Dunn ME, Larson NM, Leal LC, Carlson AD, Block RC, Briggs JB, Cheng ET, Huria HC, Zerkle ML, Kozier KS, Courcelle A, Pronyaev V, van der Marck SC (2006) ENDF/B-VII.0: next generation evaluated nuclear data library for nuclear science and technology. Nucl Data Sheets 107:2931–3060
77. Shibata K, Iwamoto O, Nakagawa T, Iwamoto N, Ichihara A, Kunieda S, Chiba S, Furutaka K, Otuka N, Ohasawa T, Murata T, Matsunobu H, Zukeran A, Kamada S, Katakura J (2011) JENDL-4.0: a new library for nuclear science and engineering. J Nucl Sci Tech 48(1):1–30
78. Koning AJ, Avrigeanu M, Avrigeanu V, Batistoni P, Bauge E, Bé MM, Bem P, Bernard D, Bersillon O, Bidaud A, Bouland O, Courcelle A, Dean CJ, Dos-Santos-Uzarralde P, Duchemin B, Duhamel I, Duijvestijn MC, Dupont E, Fischer U, Forrest RA, Gunsing F, Haeck W, Henriksson H, Hogenbirk A, Huynh TD, Jacqmin R, Jouanne C, Keinert J, Kellett MA, Kodeli I, Kopecky J, Leeb H, Leichtle D, Leppanen J, Litaize O, Lopez Jimenez MJ, Mattes M, Menapace E, Mills RW, Morillon B, Mounier C, Nichols AL, Noguere G, Nordborg C, Nouri A, Perel RL, Pereslavtsev P, Perry RJ, Pescarini M, Pillon M, Plompen AJM, Ridikas D, Romain P, Rugama Y, Rullhusen P, de Saint Jean C, Santamarina A, Sartori E, Seidel K, Serot O, Simakov S, Sublet JC, Tagesen S, Trkov A, van der Marck SC and Vonach H (2007) The JEFF evaluated data project. In: Proceeding of the international conference on nuclear data for science and technology, Nice, France 721 (EDP Sciences, 2008)
79. Ge ZG, Zhuang YX, Liu TJ, Zhang JS, Wu HC, Zhao ZX, Xia HH (2011) CENDL-3.1: the updated version of Chinese evaluated nuclear data library. J Korean Phys Soc 59(2):1052–1056
80. Ding D-Z, Guo T-C (1978) HSJ-77106, Review of U-238 capture cross-sections-En = 1–20 MeV
81. Tan V, Canh Hai N, Trong Hiep N, (1996) INDC (VN)-8
82. Browne E, Firestone RB (1986) In: Shirley VS, Firestone RB, Ekstrom LP (eds) Table of radioactive isotopes, Wiley, New York (Version 2.1 http://ie.lbl.gov/toi/index.asp)
83. Blachot J, Fiche Ch (1981) Table of radioactive isotopes and their main decay characteristics. Ann Phys 6(1981):3–218
84. Chart of Nuclides, National Nuclear Data Center, Brookhaven National Laboratory, based on ENSDF and the Nuclear Wallet Cards: http://www-nndc.bnl.gov/chart/
85. The international Reactor Dosimetry File: IRDF (2002) Nuclear data section, international atomic energy agency
86. Broom K (1964) Phys Rev 133:B874–B883
87. Rajagopalan M, Pruys HS, Grutter A, Hermes EA, von Gunten HR (1976) J Inorg Nucl Chem 38:351–352